Codeposition of nanocrystalline aluminides on a copper substrate

I. MANNA*, P. P. CHATTOPADHYAY, B. CHATTERJEE, S. K. PABI
Metallurgical and Materials Engineering Department, Indian Institute of Technology, Kharagpur, W. B. 721302, India
E-mail: imanna@metal.iitkgp.ernet.in

The present study concerns codeposition of nanocrystalline aluminide particles ($NbAl_3$ and Cu_9Al_4) along with electrodeposition of Cu on a Cu substrate. It is shown that the success of codeposition primarily depends on the selection of an appropriate electrolyte. Following codeposition under an optimum deposition condition, the microstructure, phase identity and composition of the deposit layer have been studied. In addition, microhardness and electrical resistivity of the deposit have been determined. A suitable correlation of the microstructure and composition of the deposit with its properties suggests that codeposition of $NbAl_3$ is more effective in enhancing the hardness. However, codeposition beyond a limit adversely affects the electrical conductivity. The optimum conditions for codeposition to enhance hardness without adversely affecting conductivity have been determined. Finally, it is predicted codeposition could be a suitable technique for developing a surface composite microstructure with uniform distribution of nanocrystalline aluminide particles. © *2001 Kluwer Academic Publishers*

1. Introduction

Copper is widely used as electrical and thermal conductors due to its very high conductivity [1]. However, pure Cu possesses a poor wear and oxidation resistance which pose difficulties like short circuiting in electrical contacts. Addition of Sn, Zn, Al, etc. to the bulk is known to improve the wear and oxidation resistance of Cu, though, deteriorating the electrical conductivity in the process. However, wear and oxidation are surface dependent degradation. Therefore, tailoring the surface microstructure and/or composition of the near-surface region of Cu based conductors may achieve the required protection against wear and oxidation without deteriorating the electrical and thermal conductivity of Cu. Recently, attempts have been made to introduce Cr on the surfaces of Cu by laser surface alloying to enhance the wear resistance of the substrate [2, 3]. Besides laser surface alloying, electrochemical codeposition of ceramic particles (e.g., Al_2O_3) on metal surfaces (like Cu and Ni) has recently been attempted to develop few micrometer deep composite microstructure on the surface [4]. The finer the particles, the more uniform distribution of these particles on the codeposited surface. Subsequently, it is reported that mechanical properties of the metallic substrate with such a composite surface microstructure are remarkably improved in comparison to that of the bulk [5]. However, dispersion of the insulators like Al_2O_3 may deteriorate the conductivity of the codeposited layer in applications like electrical contacts, conducting springs, etc. On the other hand, dispersion of the ultra-fine intermetallic

compounds on the surface by codeposition has significantly improved the superficial mechanical properties of Cu without any detriment to the electrical conductivity of the material [6]. However, ultra-fine particles are prone to chemical reactions. In fact, attempts to deposit other aluminides (say, Cu_9Al_4) using the same medium/technique have not been successful. Therefore, the success of codeposition largely depends on finding a suitable electrolytic medium that does not chemically degrade the fine particles.

In the present investigation, an attempt has been made to enhance the wear resistance of Cu by codeposition of hard nanocrystalline aluminide particles (namely, $NbAl_3$ and Cu_9Al_4) along with electrodeposition of Cu on pure Cu substrates. Following codeposition a detailed characterization of the surface microstructure, composition, hardness and electrical conductivity has been undertaken. Finally, an attempt has been made to compare the codeposited microstructure and improvement of the surface properties of Cu following codeposition of Cu_9Al_4 vis-á-vis $NbAl_3$ using different electrolytes and conditions of deposition.

2. Experimental

Nanocrystalline $NbAl_3$ was synthesized by MA of a stoichiometric amount ($Nb_{25}Al_{75}$) of elemental Nb and Al powders (>99.5% purity) having an average particle size of 100 μm in a Fritsch P5 planetary ball mill in hardened chrome steel vials and balls rotating at a disc speed of 300 rpm at a ball to powder weight ratio

of 10 : 1. Similarly, MA of a Cu-Al powder blend with the required initial composition was carried out in the same device under similar milling conditions for up to 20 h. Subsequently, the as milled powder was subjected to isothermal annealing at 200°C for 2 h. The as milled and/or annealed powders were collected at appropriate stages to determine the identity and average crystallite diameter (d_c) through x-ray diffraction (XRD) using a Phillips PW 1840 diffractometer with Co-K_α (0.179 nm) radiation. d_c was calculated through a peak broadening analysis based on Scherrer equation [7] after suitable elimination of strain and instrumental broadening effects [8].

Initial trials revealed that nanocrystalline NbAl$_3$ remained unreacted while Cu$_9$Al$_4$ dissociated to form Al$_2$O$_3$ and Cu when dispersed and suspended in CuSO$_4$ solution for over 10 h (i.e., a typical codeposition time). Subsequent attempts showed that mildly acidic aqueous solution of Cu(CH$_3$COO)$_2$ was suitable for the dispersion and codeposition of Cu$_9$Al$_4$ along with the electrodeposition of Cu on Cu cathodes without any chemical change of Cu$_9$Al$_4$ suspended in the Cu(CH$_3$COO)$_2$ solution. Therefore, an acidified CuSO$_4$ bath (with a pH level of 3.5–4.0) was used for codeposition of the suspended NbAl$_3$ nano-particles along with electrodeposition of Cu on flat Cu plates. On the other hand, codeposition of Cu$_9$Al$_4$ was carried out in a mildly acidic bath (with a pH level of 5.0–5.5) prepared by dissolving Cu(CH$_3$COO)$_2$ in an aqueous medium with the same electrodes as that used for the CuSO$_4$ bath. The electrodeposition was carried out at a d.c. potential of 3–5 and 1-2 volts applied between the Cu-cathode and Pt-electrode for CuSO$_4$ and Cu(CH$_3$COO)$_2$ baths, respectively. In both the cases, the baths were maintained at 40°C using a thermostat. The uniformity of the dispersion of particles was maintained by magnetic stirring prior to (for 30 min) and during electrodeposition. The process parameters varied were time (t), current (i) and dispersion weight (w) of the powder particles. Table I summarizes the process parameters used for codeposition of NbAl$_3$ and Cu$_9$Al$_4$.

Following codeposition under predetermined routines, the samples were subjected to a detailed characterization in terms of the surface microstructure (by scanning electron microscopy, SEM), surface chemistry (by energy dispersive spectroscopy, EDS), and phase identity (by XRD). Superficial hardness of the codeposited samples was determined by using Vickers microhardness tester with 50 g applied load. The average microhardness was determined from the automatic recorder from the width of the indentation diagonals as per the equation:

$$H_v = (1854.4 \times L)/d_w^2 \qquad (1)$$

where, H_v is the microhardness in kg/mm^2, L is the applied load in g, and d_w is the average diagonal width in μm.

Subsequently, a selected set of samples, prepared by codeposition of the chosen nano-aluminide particles with Cu on transparent silica substrates pre-coated by physical vapor deposition with a 1 μm thick Cu film was subjected to electrical resistivity measurements by the four probe direct current Double Kelvin Bridge method. For these measurements, the dependence on geometry and sensitivity to the boundary conditions was normalized by adopting the Van der Pauw method of correction [9]. Finally, an attempt has been made to correlate the conductivity and hardness with the microstructure and composition of the surface layer.

3. Results and discussion
3.1. Synthesis of intermetallic phases
Fig. 1 shows the evolution of the ordered NbAl$_3$ phase during planetary ball milling of an elemental blend of Nb and Al powders. It is found that d_c of NbAl$_3$ is reduced to below 10 nm after 30 h of ball milling (calculated from the broadening of the (112)$_{NbAl3}$ peak). However, XRD patterns obtained from the Cu$_{67}$Al$_{33}$ powder blend after prolonged ball milling indicate that MA yields a metastable bcc phase rather than the desired ordered intermetallic compound (Fig. 2). In order to obtain the ordered Cu$_9$Al$_4$ phase, the ball milled product (for $t = 20$ h) was subjected to an isothermal annealing treatment at different tremperatures for a reasonable duration of time (2 h). Subsequent XRD analyses reveal that isothermal annealing at 200°C for 2 h produces an almost identical pattern as that after annealing at 400°C for 2 h. Hence, annealing at 200°C appears capable of transforming the metastable bcc phase to the ordered Cu$_9$Al$_4$ phase with $d_c \approx 65$ nm (Fig. 2).
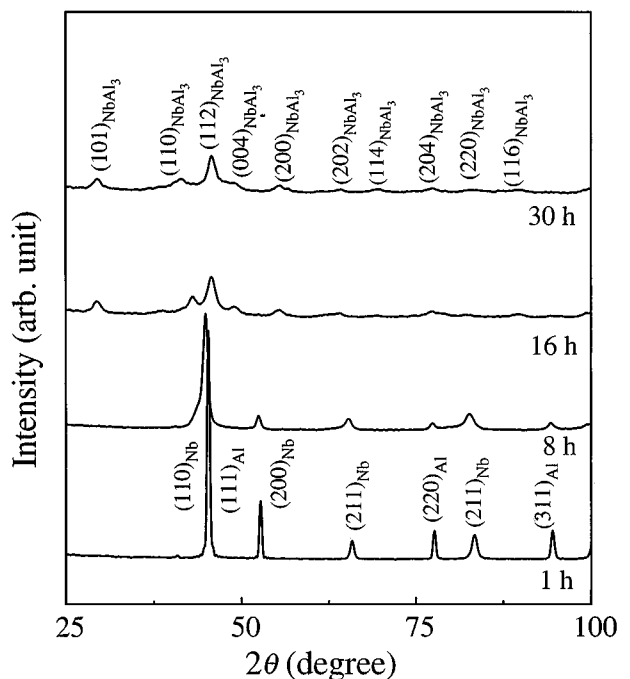
TABLE I Codeposition parameters used in the present experiment

Electrolyte	Cathode	Intermetallic phase	pH	Current (A)	Stirrer speed (rpm)
CuSO$_4$	Cu	Nb$_3$Al	3.5–4.0	3.0–4.0	50–70
Cu(CH$_3$COO)$_2$	Cu	Cu$_9$Al$_4$	5.0–5.5	0.5–1.0	25–30

Figure 1 XRD patterns obtained from a Nb$_{25}$Al$_{75}$ powder blend following ball milling for different periods of cumulative time.

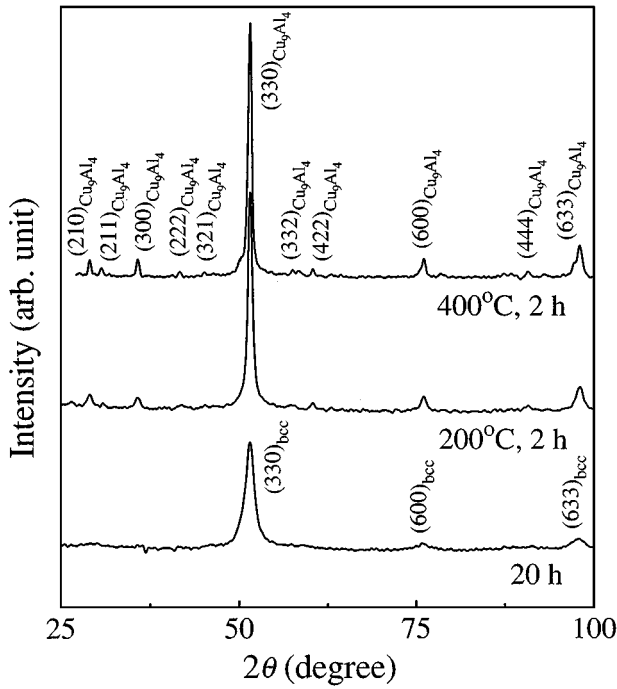*Figure 2* XRD patterns obtained from a $Cu_{67}Al_{33}$ powder blend following ball milling for 20 h and subsequent isothermal annealing (for 2 h) at different temperatures.

3.2. Codeposition of intermetallic particles

Initial trials in the present experiment reveal that the relative rate of electrodeposition of Cu and codeposition of the nano-particles is crucial to obtain a smooth and adherent deposit layer on the surface. While electrodeposition is a strong function of i, codeposition is primarily dictated by w and uniformity of dispersion of the nano-particles. Therefore, w must have an upper limit for any given i, beyond which accumulation of excess particles on the cathode may hinder the electrochemical process of ionic charge transfer between the cathode and Cu ions. Earlier, it has been shown that the ratio of mass of electrodeposited Cu to that of codeposited NbAl$_3$ particles remain typically at 1.8 under the condition of maximum density of codeposition [6]. Assuming a similar condition that the codeposited spherical nano-particles are in contact with each other and electrodeposited Cu atoms are embedded in the interstitial spaces of those nano-particles, a simple arithmetic calculation yields

$$\frac{m_{Cu}}{m_P} = 0.9 \frac{\rho_{Cu}}{\rho_P} \qquad (2)$$

where, the subscripts Cu and P to the mass (m) and density (ρ) terms related to Cu and the nano-particles, respectively. Thus, the deposited mass is proportional to the concerned density. Fig. 3 presents a variation of the theoretically determined values of the total electrodeposited mass ($m_t = m_{Cu} + m_P$) as a function of t for codeposition of both NbAl$_3$ and Cu$_9$Al$_4$ particles. For a suitable comparison, the experimentally determined values of m_t in the cases of NbAl$_3$ and Cu$_9$Al$_4$ are included in Fig. 3. It is apparent that the predicted rate is closer to the experimentally determined deposition kinetics in the case of codeposition of Cu$_9$Al$_4$.
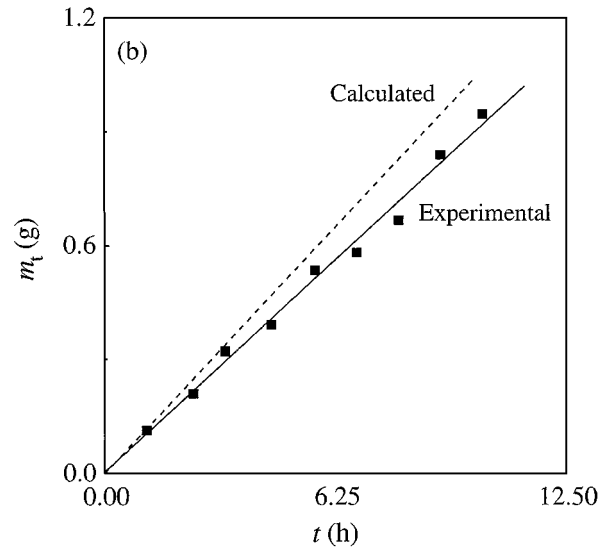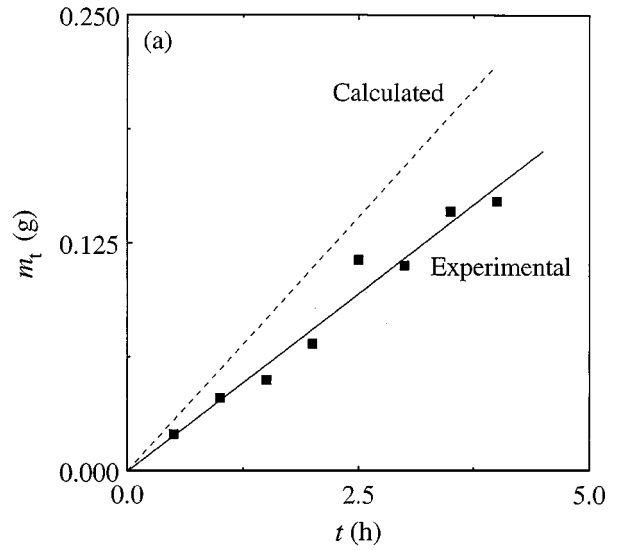

Figure 3 Variation of accumulated mass (m_t) obtained by codeposition of (a) NbAl$_3$ and (b) Cu$_9$Al$_4$ particles dispersed within the electrodeposited Cu matrix as a function of codeposition time.

However, the higher the t, the greater the difference between the theoretically predicted and experimentally determined values of m_t in both the cases of codeposition. This difference may be attributed to the gradual dilution of Cu-ions and nano-particles in the solutions with the progress of electro/codeposition. Thus, Equation 2 may be useful to calculate the amount of nano-particles to be suspended in the electrolyte to obtain the required m_p for a given condition of codeposition.

3.3. Microstructure and composition of the deposit

Following codeposition, a microstructural investigation of the codeposited surface has been conducted to reveal the distribution of the codeposited particles on the surface of the substrates. Fig. 4 reveals a typical scanning electron micrograph of the surface of a Cu substrate codeposited with NbAl$_3$ powders. It is evident that NbAl$_3$ is mostly deposited along the boundaries of electrodeposited Cu grains. However, Fig. 4 also
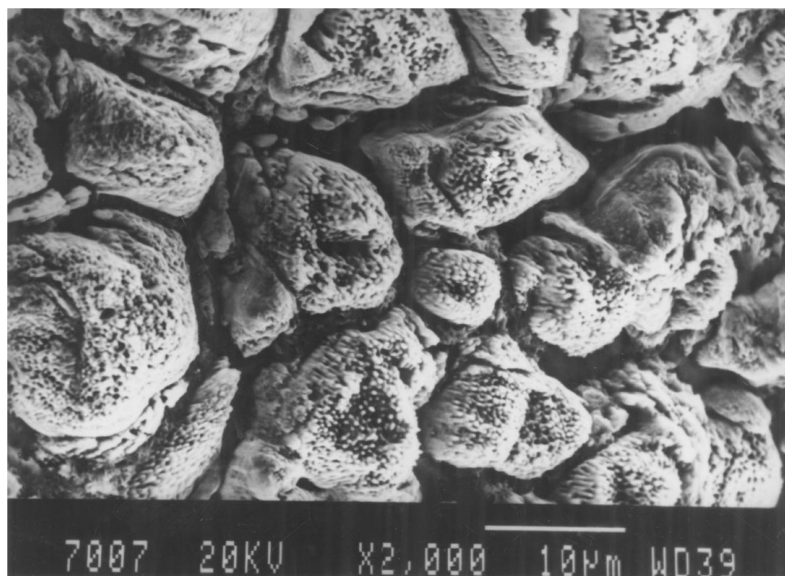
Figure 4 SEM micrograph showing the distribution of NbAl₃ particles along the grain boundary as well as within the bulk.

evidences entrapment of NbAl$_3$ particles both along the grain boundaries and within the grain bodies. The NbAl$_3$ particles tend to agglomerate into coarser aggregate of nearly micrometer sizes during codeposition. These morphological features are in accordance with the earlier reported study of codeposition of NbAl$_3$ on Cu [6].

Similar scanning electron micrographs of the Cu surface codeposited with Cu$_9$Al$_4$ are shown in Figs 5 and 6. Here, the Cu$_9$Al$_4$ particles, in addition to segregating in the interdendritic spaces, get entrapped on the tips of the advancing Cu-dendrites in large quantity. It is interesting to note that the morphologies of deposited composite layers obtained by codepositing NbAl$_3$ (equi-axed) using the CuSO$_4$ electrolyte (Fig. 4) and codepositing Cu$_9$Al$_4$ (dendritic) using the Cu(CH$_3$COO)$_2$ electrolyte (Figs 5 and 6) are distinctly different. Perhaps, the influence of the concerned electrolyte on the interfacial energy is responsible for developing the different growth morphologies of the deposit.

It may be mentioned here that the interface between the deposit and underlying substrate is quite sharp both in terms of microstructure and composition. However, the deposit is well compatible with the substrate and is devoid of any noticeable defect (crack or porosity) in either cases of codeposition.

Figs 7 and 8 confirm the presence of NbAl$_3$ and Cu$_9$Al$_4$ in the codeposited surface of Cu through a careful XRD analysis of the codeposited samples. It may be noted that the intensity distribution of the Cu peaks shown in Fig. 7 for codeposition of NbAl$_3$ from CuSO$_4$ bath is different than those in Fig. 8 obtained from a sample with codeposition of Cu$_9$Al$_4$ from Cu(CH$_3$COO)$_2$ bath. In the former, the peak intensities (I) are decreasing in the order of $I_{220} < I_{200} < I_{111}$, while in the latter, the intensity distribution follows that recorded in the standard powder diffraction profile (i.e. $I_{111} > I_{200} > I_{220}$). Such a difference may be attributed to the development of pronounced texture during electrodeposition of Cu.
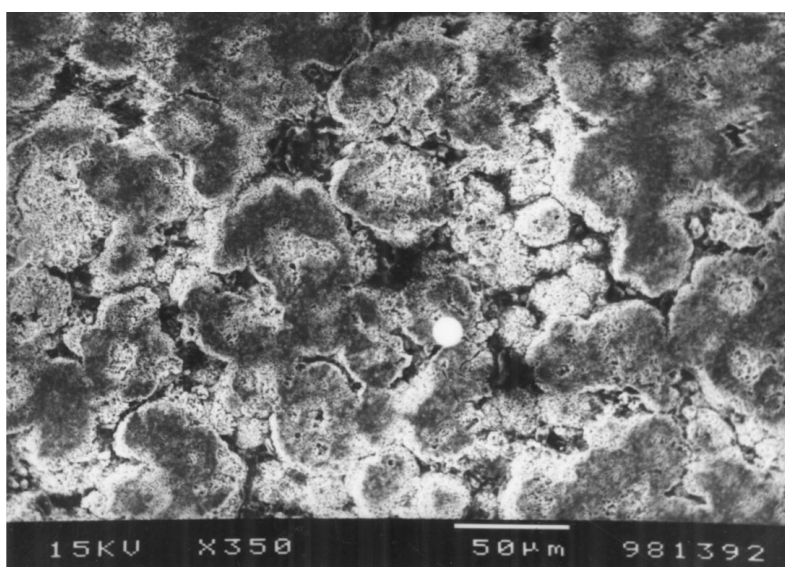

Figure 5 SEM micrograph showing the dendritic morphology of the electrodeposited Cu with codeposited Cu$_9$Al$_4$ particles embedded on it.
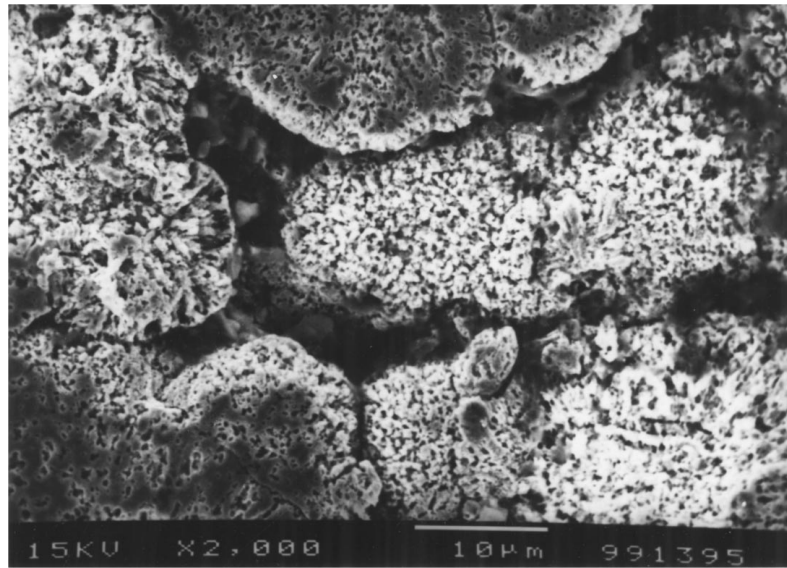
1422

Figure 6 SEM micrograph showing the distribution of Cu_9Al_4 particles in the interdendritic region as well as within the dendrites.
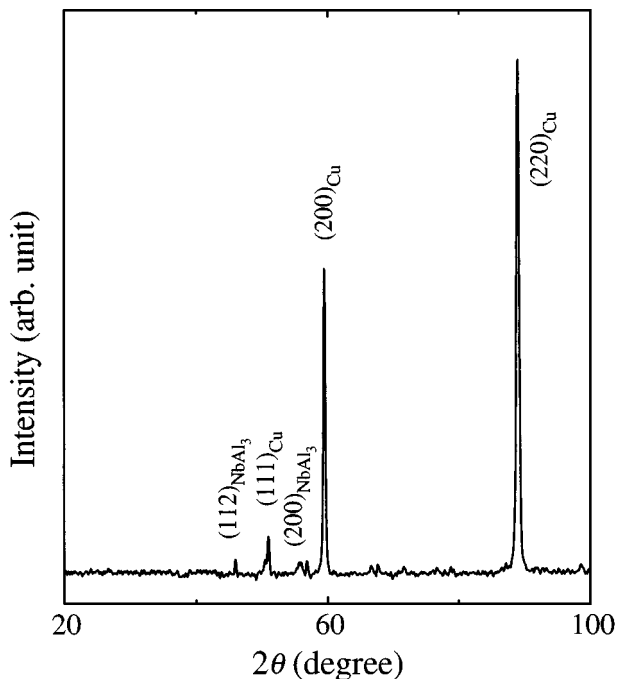

Figure 7 XRD pattern of codeposited surface showing the presence of the $NbAl_3$ particles dispersed in the electrodeposited Cu matrix.
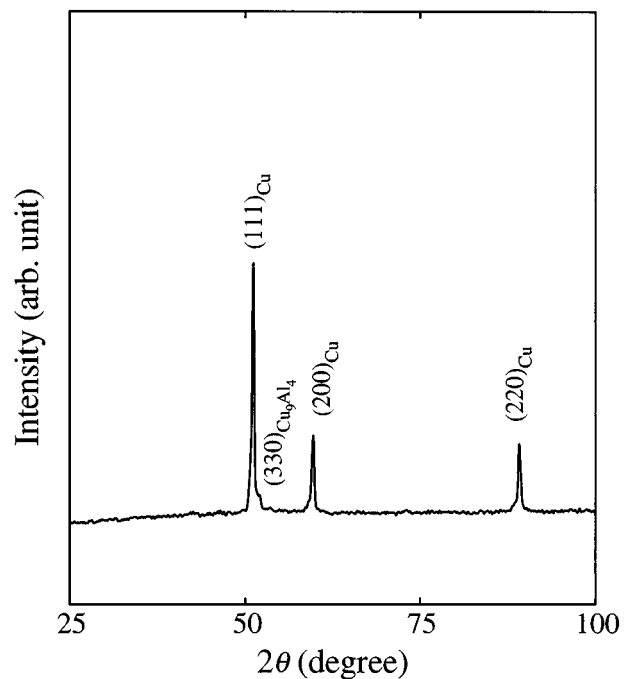

Figure 8 XRD pattern of codeposited surface showing the presence of the Cu_9Al_4 particles dispersed in the electrodeposited Cu matrix.

A selective EDS analysis reveals the presence of Cu, Nb, Al, Cr and Fe in randomly chosen areas of the surface deposits containing $NbAl_3$. Fe and Cr may be the impurities introduced during ball milling. A typical analysis result shows: Cu-40.52, Nb-11.68, Al-36.15, Cr-2.89 and Fe-8.76 (all in at.%). This result further confirms that Nb and Al are present in the surface deposit as $NbAl_3$ (Nb : Al $= 11.68 : 36.15 \approx 1 : 3$). A similar EDS analysis of several spots on the Cu-surface codeposited with Cu_9Al_4 reveals an average composition of Cu-71.0, Al-26.45, Cr-0.64 and Fe-1.92. In the case of codeposition of Cu_9Al_4 the presence of the latter could not be confirmed from the results of EDS analysis as Cu is a part of both the dispersoid and matrix. It may noted that the presence of Fe and Cr in both the codeposited surfaces indicates that these elements are the impurities picked up during MA using the hardened steel media in the planetary ball mill.

3.4. Properties of the codeposited surface

Table II summarizes the mechanical (hardness, H_v) and electrical (resistivity) properties of the surface deposits for different density of dispersion in the electrolyte during codeposition of both $NbAl_3$ and Cu_9Al_4. It is apparent that the average H_v (taken from several regions of the surface deposit) of the co-deposited $NbAl_3$ samples registers a 2.5–4 fold increase than that of the pure Cu substrate. In addition, it is further interesting to note that the resistivity of the co-deposited $NbAl_3$ samples remains nearly identical (same order of magnitude) as that of pure Cu. At higher volume fraction of $NbAl_3$,

TABLE II Results of hardness and electrical resistivity measurements

Sample	Particles (g/l)	H_v (VHN)	Resistivity (Ωcm)
Pure Cu	—	84	1.6×10^{-6}
	2	215	7.8×10^{-6}
Cu/NbAl$_3$	3	293	8.9×10^{-6}
	4	340	1.1×10^{-5}
	2	171	2.6×10^{-6}
Cu/Cu$_9$Al$_4$	3	177	3.9×10^{-6}
	4	195	7.0×10^{-6}

however, resistivity is an order of magnitude higher than that of pure Cu. Similar results are also obtained in the case of codeposition of Cu$_9$Al$_4$. Here, approximately a two fold increase in hardness is obtained indicating a marginal improvement of mechanical property of the co-deposited surface in comparison to that due to the dispersion of NbAl$_3$ particles. However, it may be mentioned that an increase in H_v with higher than a critical amount or density of NbAl$_3$ or Cu$_9$Al$_4$ may adversely affect the conductivity of the codeposited surface.

Finally, it is relevant to mention that a similar codeposition of nano-particles is, in principle, feasible on other substrates like Ni, Fe, Al or their alloys, provided a suitable electrolyte is found which doesn't chemically react with the chosen nano-particles. In view of the high reactivity and grain coarsening tendency of nano-particles in any thermally activated process, codeposition is a promising route of utilizing nanocrystals for developing a superficial composite coating on engineering components to enhance resistance to wear, corrosion and similar surface dependent degradation.

4. Conclusions

1. It is demonstrated that codeposition of nanocrystalline NbAl$_3$ and Cu$_9$Al$_4$ on Cu substrates is feasible under the optimum conditions of electrodeposition of Cu defined in this study.

2. A detailed characterization of the surface microstructure and composition reveals that nanocrystalline NbAl$_3$ is uniformly distributed as individual and agglomerated particles along the grain bodies and boundaries, while Cu$_9$Al$_4$ nano-particles are dispersed within the dendritic arms and interdendritic spaces of electrodeposited Cu, respectively.

3. A mathematical expression is proposed to determine the approximate ratio of the relative amounts of the electrolyte and particles to be dispersed in the electrolyte for the given values of deposition current, duration and dispersion density.

4. It appears that the selection of a proper electrolyte is the most important criterion for the successful codeposition of a chosen intermetallic compound. Furthermore, the growth morphology may widely differ for the same substrate and electrodeposited metal during the codeposition process if the electrolytes are different.

5. It is demonstrated that average microhardness of Cu increases by 2.5–4 fold under the suitable conditions of codeposition without adversely affecting its electrical conductivity. Codeposition of NbAl$_3$ appears to be more effective than Cu$_9$Al$_4$ in improving the hardness of the codeposited copper surface in comparison to that of the bulk.

6. The codeposited nano-aluminide dispersed composite coating seems well adherent and compatible with the underlying substrate.

References
1. E. G. WEST, in "Copper and its Alloys" (Ellis Harwood, Chichester, 1982) p. 125.
2. I. MANNA, J. DUTTA MAJUMDAR, U. K. CHATTERJEE and A. K. NATH, *Scr. Metall. Mater.* **35** (1996) 405.
3. J. DUTTA MAJUMDAR and I. MANNA, *Mater. Sci. Eng.* **A268** (1999) 219 and 227.
4. R. R. OBERLE, M. R. SCANION, R. C. CAMMARATA and P. R. SEARSON, *Appl. Phys. Lett.* **66** (1995) 19.
5. X. M. DING, N. MERK and B. ILSCHNER, *J. Mater. Sci.* **33** (1998) 803.
6. I. MANNA, P. P. CHATTERJEE and S. K. PABI, *Scr. Metall Mater.* **40** (1999) 409.
7. B. D. CULLITY, in "Elements of X-ray Diffraction" (Addison Wesley, MA, 1975) p. 102.
8. I. L. LANGFORD, *J. Appl. Cryst.* **11** (1978) 10.
9. A. A. RAMADAN, R. D. GOULD and A. ASHAUR, *Thin Solid Films* **239** (1994) 272.